Accepted manuscript doi:
10.1680/jgein.20.00030

Accepted manuscript doi:
10.1680/jgein.20.00030

Submitted: 02 March 2020

Published online in 'accepted manuscript' format: 23 July 2020

Manuscript title: Repeated loading of soilbag-reinforced road subgrade

Authors: S. H. Liu[1], J. Liao[1], T. T. Bong[1] and K. W. Fan[1,2]

Affiliations: [1]College of Water Conservancy and Hydropower Engineering, Hohai University, Nanjing 210098, China and [2]School of Civil Engineering, Wuhan University, Wuhan 430072, China

Corresponding author: J. Liao, College of Water Conservancy and Hydropower Engineering, Hohai University, Nanjing 210098, China.

E-mail: liaojiehhu@gmail.com

Accepted manuscript doi:
10.1680/jgein.20.00030

Abstract

Soilbags are three-dimensional soil-confining units used in road foundations. This paper uses vertical repeated loading tests to investigate the performance of soilbags as reinforcement in road subgrades as well as the influence of such factors as the frequency and amplitude of loading, the number of reinforcement layers, and the buried depth of the soilbag reinforcement. The results show that soilbags as reinforcement are effective at reducing permanent and resilient deformations of the road subgrade as well as vibrations caused by traffic loads. The soilbags as reinforcement perform better when the number of soilbag-reinforced layers is increased. More than two layers of soilbags are needed to reinforce the road subgrade to make efficient use of the effect of interlayer insertion between soilbags. Furthermore, a thin surface soil cover is desirable to spread the applied pressure more effectively over the soilbags and level the subgrade.

Keywords: Geosynthetics; Soilbags; Subgrade reinforcement; Repeated loading tests; Deformation; Acceleration

Accepted manuscript doi:
10.1680/jgein.20.00030

1. INTRODUCTUION

Polythene (PE) and polypropylene (PP) bags filled with soil are commonly used to prevent the flow of soils due to floodwater by building temporary emergency structures, rather than reinforced earth embankments Studies by Matsuoka and Liu (1999, 2003, 2006) have revealed many engineering-related properties of soilbags, such as environmental friendliness, ability to improve the bearing capacity of soft ground, reduce traffic-induced vibrations, and prevent frost heave. Polythene (PE) and polypropylene (PP) bags protected from exposure to sunlight (via burial) are known to be durable. Due to these attributes, soilbags have also been used in permanent or semi-permanent projects as reinforcements for soft soil foundations (Matsuoka and Liu, 2006; Liu and Matsuoka, 2007; Xu et al. 2008; Li et al. 2013), expansive soil treatment (Liu et al. 2013, 2015; Wang et al. 2015), constructing retaining walls (Lee et al. 2013; Wen et al. 2016; Liu et al. 2019, Fan et al. 2019, Wang et al. 2019a, b), coastal protection projects (Martinelli et al. 2011; Hornsey et al. 2011; Kim et al. 2015; Moreira et al. 2016), and for improving road foundations (Matsuoka and Liu, 2006; Indraratna et al. 2014; Liu et al. 2017). There are three major advantages of using soilbags in road foundations: 1) an increase in the bearing capacity of the road subgrade, 2) a decrease in deformation, especially in uneven settlement along the road, and 3) a reduction in traffic-induced vibrations on the ground. For example, Matsuoka and Nomoto (2008) reported on the construction of a 25-m-long highway with soilbags containing 3~4-m-thick layers of clay supporting the foundation. The bearing capacity of the reinforced subgrade using plate loading tests was calculated to be 224 N/cm^2 (greater than the design value of 180 N/cm^2), and the settlement measured after 10 months of operation was 2 cm. Shao et al. (2005) used soilbags to fill ponds to construct a highway embankment and reduce the settlement of the subgrade. The increase in the bearing capacity and a decrease in the deformation of the road subgrade result from the high strength and confinement of the soilbags (Matsuoka and Liu, 2006; Cheng et al. 2016; Liu, 2017). Wang et al. (2019) investigated the bearing capacity of soilbag-reinforced foundations by conducting field load tests and numerical analysis using the finite element method (FEM). They found that the bearing capacity of the reinforced soft foundations improved, and settlement decreased with increasing number of soilbags used as reinforcement due to stress dispersion. Tantono and Bauer (2008) claimed that interfacial friction between the soil and the bag can have a strong influence on the bearing capacity of the elements of the bags. The effectiveness of soilbags at reducing traffic-induced vibrations was first noted in their use in the foundations of a railway ballast in a Japanese railway line (Matsuoka et al. 2000; Matsuoka and Liu, 2003). The measurements in the case study showed that the average acceleration of oscillation of the trains decreased from

0.12 g to 0.04 g after the foundation had been reinforced by soilbags, accompanied by a reduction in the settlements of railway sleepers to less than 10 mm. The efficiency of soilbags in terms of reducing traffic-induced vibrations has been verified further through field tests (Matsuoka et al. 2002, 2003; Matsuoka and Ando, 2006; Nakagawa et al. 2009). The results showed that the vibrations of 5~15 dB could be reduced after reinforcement by soilbags. Based on an FEM simulation of a field test, Ye et al. (2011) numerically evaluated the vibration damping effect of soilbags and concluded that it relies heavily on the position of the source of the vibration. The dynamic properties of stacked soilbags have been studied through a series of cyclic lateral shear tests (Yamamoto et al. 2003; Liu et al. 2014), and an "equivalent damping ratio" was introduced to evaluate the reduction in vibrations induced by soilbags. They were found to have a relatively high damping ratio and variable horizontal stiffness that are significantly influenced by the infill material at a low vertical stress but become nearly independent of it at a high vertical stress (Wang et al. 2019). Wang and Wang (2014) used the discrete element method (DEM) to investigate the reduction in vibration brought about by a soilbag by developing an energy dissipation equation. The results showed that a high percentage of the surface of the soil-bag and the particles inside it absorbed energy in the form of wave-shaped fluctuations during loading and unloading. The effect of the reduction in vibrations and factors influencing this have also been investigated through vertical excitation tests and small shaking table tests (Liu et al. 2014). The vertical excitation tests were performed both on vertically piled soilbags in a box and on soilbags layered on hard ground in two types of arrangements. The results showed that three or four layers of soilbags placed near the source of the vibrations significantly damped them, and their staggered arrangement was more effective than an in-line arrangement at reducing vertical vibrations.

However, the above-mentioned studies have not considered conditions related to traffic loads, which are crucial to the status of roads. Traffic loads induced by moving vehicles, acting on roads in a short time with a high intensity of impulse, are commonly simulated under vertical repeated loading. For example, Suku et al. (2017) investigated the effects of geogrid reinforcements on pavement bases by using repeated plate load tests. Similarly, Tafreshi et al. (2014) carried out a series of repeated plate load tests to assess geocell-reinforced layers and layers of rubber–soil mixture as means of improving the foundation of pavements. Recently, Ding et al. (2017, 2018) investigated the reduction in vibrations and deformation brought about by using soilbags in road and railway subgrades by carrying out a series of laboratory tests under repeated loading applied by three spaced exciters (hydraulic jacks with phase-shifted excitations). The influence of different filling materials in

woven bags, the location of the source frequency, and the number of exciters on the reduction in vibration was investigated.

This study investigates the effect of soilbags used in road subgrades in terms of reducing vibrations and settlement under traffic loads through experiments involving repeated loading. It is different from previous studies in the area in that it reports the results of vertical repeated plate load tests on a model subgrade with a localized reinforcement provided by soilbags, instead of purely stacked soilbags. The effects of the frequency and amplitude of cyclic loading, the number of layers of soilbags, and their embedded depths on vibrations and settlement were examined.

2. REPEATED PLATE LOAD TESTS

2.1 Test apparatus

The test apparatus, as shown in Figure 1, featured a loading system, a testing tank, and a data acquisition system. The loading system consisted of a reaction frame, a pneumatic cylinder, and a controlling unit. The reaction frame comprised two stiff and heavy steel columns 1300 mm high and a horizontal beam 3000 mm long that supported the pneumatic cylinder. The cylinder could produce monotonic or cyclic loads depending on the intensity of the input compressed air. Cyclic vertical loads of different magnitudes (up to 800 kPa), frequencies (up to 5 Hz), and numbers of load cycles could be produced and controlled by the cylinder. The controlling unit consisted of an electro-mechanical valve to regulate the intensity of the compressed air required to produce a cyclic load of the desired amplitude and frequency. The model tank was designed as a rigid box measuring 1200 × 800 mm in plane and 750 mm in height. To allow for the visual observation of the subgrade reinforcement system as well as photo-scanning, the front face of the model box was made of a 10-mm-thick plexiglass. The rigidity of the model tank was guaranteed by using a stiff steel section U-100 on four sides of the box. A circular plate 200 mm in diameter and 20 mm thick was used to transfer repeated loads onto the base. A load cell was connected to the piston of the actuator to measure static/dynamic loads. Two linear variable differential transformers (LVDTs) with an accuracy of 0.01% at full range (70 mm) were positioned on top of the circular plate to measure its settlement due to loading. The vibration response of the road subgrade model under repeated loading was measured by acceleration sensors installed at different depths of the subgrade model and on the surface away from the circular load plate at different distances. The load cell, LVDTs, and acceleration sensors were all connected to a dynamic signal acquisition system for data acquisition. To ensure an accurate reading, all devices, especially the displacement transducers, were calibrated prior to each test.

2.2 Test materials

River sand with grain sizes ranging from 0.06 mm to 5 mm was used in the subgrade and as infilling for the soilbags. The sand was characterized per ASTM standards, and its properties are given in Table 1.

White woven bags, made of polypropylene with a weight per square meter of 70 g, were used as wrapping material for the soilbags, and had longitudinal and transverse tensile strengths of 11.6 kN/m and 5.2 kN/m, respectively. The maximum elongation in the warp and weft directions was 25%. Around 30 kg of sand was used to fill each bag, and the mouth of the bag was sealed with a portable sewing machine. After compaction, each soilbag had approximate dimensions of 40 cm × 40 cm ×10 cm.

Commercially available biaxial geogrids were used as contrast reinforcement materials in the experiment. The geogrids comprised polypropylene with a square aperture opening of 40 mm × 40 mm. The ultimate tensile strength of the geogrid was 15.8 kN/m while its mass per unit area was 300 g/m2. The standard longitudinal and transverse elongations were less than 12.8% and 11.6%, respectively.

2.3 Experimental program

In-box cyclic plate load tests were conducted in the laboratory to investigate the benefits of using soilbags as localized reinforcement in road subgrades. For comparison, tests were also conducted on an unreinforced subgrade and a geogrid-reinforced subgrade. Twelve tests in different series were planned and carried out to quantify the effectiveness of the soilbag-reinforced subgrade, and to study the effects of the amplitude and frequency of the dynamic load, number of reinforced layers, and the buried depth of soilbags on the behaviour of the road subgrade model. Table 2 gives the testing arrangement used in this study. A schematic layout of the model along with the positions of the acceleration sensors and the LVDTs, in case of reinforcement consisting of three layers of soilbags and geogrids, are shown in Figure 2. As vibration damping by the soilbags was more effective in a staggered arrangement than an inline arrangement (Liu et al. 2014), the former was employed using soilbags with dimensions of 40 cm × 20 cm ×10 cm. For each test, sand was placed in layers and compacted to a bulk density of 1.7 g/cm^3 (relative density Dr = 95%). In the geogrid-reinforced subgrade model, the anchor length of the geogrids could have affected deformation behaviour. Mehrjardi et al. (2016) conducted a series of plate load model tests (vertical loads of up to 800 kPa) and concluded that the appropriate length of the geogrid is four times the diameter of the load plate. The geogrids in this study were 1200 mm long and 800 mm wide, more than four times the diameter (200 mm) of the load plate.

The magnitude of the maximum applied repeated surface load was selected based on the Chinese code for the Design of Highway Asphalt Pavement (JTG D50-2017). The recommended axle load of the truck was 200 kN, over two pairs of twin wheels, which created a stress of approximately 700 kPa. Monismith et al. (1975) have reported that tire pressure ranging from 200 kPa to 800 kPa is relatively closer to the case for actual traffic. The applied pressures in this study were 250, 500, and 750 kPa, with each loading sequence repeated for 1,000 cycles. Traffic load has the characteristics of instantaneity and repeatability. When its impact on road structures is analysed, it is usually simplified as a repeated load with a periodically changing magnitude. Several loading forms have been used by different researchers, such as sine loading (Wang et al. 2018; Suku et al. 2016), triangular loading (Ling et al. 2002; Saad et al. 2005), half-sine loading (Hanazato et al. 1991), and rectangular loading (Thakur et al. 2012; Tafreshi and Dawson, 2010). The frequency of dynamic traffic loads varies with such factors as vehicle speed, driving density, the road foundation, and structure of the pavement. Haversine loading was applied here to the circular plate at different frequencies. The deformation in the model subgrade when subjected to repeated loading was resolved into two components—plastic and resilient. The reversible deformation was resilient deformation and non-reversible deformation was plastic deformation, where the accumulation of the latter was permanent deformation. Figure 3 shows cycles of repeated loads applied to the surface of the model subgrade as well as the consequent plastic and resilient deformations. The repeated load was returned to zero at the end of each cycle, which is typical of a vehicle on a track or pavement support.

3. RESULTS AND DISCUSSION

In this section, the results of the cyclic plate load tests are presented to gauge the effectiveness of soilbags as reinforcement, and a discussion highlighting the effects of different parameters, including the loading frequency, loading amplitude, number of reinforcement layers, and the location of the embedded soilbags, is provided. Changes in the performance of the reinforced subgrade were tested by varying the plate settlement and the distributed acceleration at a depth and the surface of the model subgrade.

3.1 Effectiveness of soilbag reinforcement

To verify the effectiveness of soilbags as reinforcement, the cyclic plate load tests were comparatively conducted on a model subgrade reinforced with three layers of soilbags and three layers of geogrids (*see* Figure 2), and on an unreinforced subgrade under a loading amplitude of 500 kPa with a frequency of 1 Hz. Figure 4(a) shows a comparison of the permanent deformation (settlement) that developed with the number of loading cycles. Three types of reinforcements showed similar trends in the settlement, that is, an abrupt increase under

the initial loading cycle followed by a slow increase to a relatively stable value with increasing number of cycles. The abrupt increase was related to the densification of the model subgrade under initial cyclic loading. It is evident that soilbags used as reinforcement led to the lowest settlement and the least cycles, in accordance with the abrupt increase in the three cases. After 1,000 cycles of loading, the settlement of the soilbag-based reinforcement was 22.23 mm, whereas those of the geogrid reinforcement and the unreinforced subgrade were 35.36mm and 67.44 mm, respectively. The large vertical displacement of the unreinforced subgrade occurred owing to the slight penetration of the load plate into the sand and the rising of its surface around the loading plate. To further investigate the effects of different types of reinforcement, the plastic deformation generated in each cycle in the initial 200 cycles is compared in Figure 4(b). It is clear that the plastic deformation was around 0.3 mm at the first loading cycle, and decreases abruptly after several cycles in case soilbags were used as reinforcement, whereas the unreinforced subgrade had a plastic deformation larger than 1 mm at the first loading cycle and a considerable reduction after 50 cycles. The plastic deformation for the geogrid reinforcement was in between these values. As the permanent deformation is the accumulation of the plastic deformation under repeated loading cycles, the abrupt decrease in the plastic deformation implied low permanent deformation and the quick stabilization of the subgrade. Soilbags when used as reinforcement led to the lowest permanent deformation and an abrupt decrease in plastic deformation in several initial cycles, which is their most desirable advantage for road pavements.

Figure 4(c) compares the resilient deformation of different types of reinforcements generated in each cycle in the initial 200 cycles. Similarly, the soilbag-based reinforcement had the lowest resilient deformation of around 0.9 mm. According to Qian et al. (2011), the resilient deformation is directly related to the resilient modulus. They carried out plate load tests on a geosynthetics-reinforced subgrade and proposed an empirical formula, Equation (1) to calculate resilient modulus.

$$E = \frac{BIq(1-\nu^2)}{\delta} \quad (1)$$

where E is the resilient modulus, B is the diameter of the loading plate, I is the influence factor, q is the pressure applied on surface of the subgrade, ν is the Poisson's ratio, δ is the resilient deformation. Equation (1) suggests that the resilient modulus is negatively correlated with the resilient deformation. If I is assumed to be 1.6 (Suku et al. 2017) and ν is 0.3, the resilient modulus of the model subgrade is in the range 165 MPa–190 MPa for the soilbag-based reinforcement, 130 MPa–150 MPa for the geogrid-based reinforcement, and 90 MPa–125 MPa in the unreinforced subgrade, based on the resilient deformations shown in Figure 4(c). The soilbag-based

reinforcement had the highest resilient modulus, which can be attributed to the stronger constraint of woven polypropylene bags as well as the interlocking effect of the soilbag interlayer, which increased anti-deformation ability and led to a reduction in resilient deformation. Figure 4 shows that the soilbag-based reinforcement had the lowest permanent, plastic, and resilient deformations under repeated loading, indicating superior performance.

The acceleration response during the cyclic plate load tests was also examined. Figure 5 shows time histories of the acceleration of the case where soilbags were used as reinforcement at different depths. The acceleration response decreased with increasing depth. The peak acceleration measured at a depth of 5 cm was 0.24 m/s^2, whereas no clear acceleration response was detected unless the load reached its amplitude at a depth of 5 cm. To evaluate the reduction in vibrations, the rate of attenuation in acceleration between two adjacent measuring points was defined (Liu et al. 2014; Ding et al. 2018).

$$AR = (a_{max}^{i-1} - a_{max}^{i})/a_{max}^{i-1} \quad (2)$$

where a_{max}^{i} and a_{max}^{i-1} are peak accelerations at the measuring points *i* and *i-1*, respectively.

Figure 6 shows a comparison of variations in peak acceleration (PA) and the rate of attenuation (AR) for different types of reinforcements in terms of depth and horizontal distance. It is evident that at the same depth of, or horizontal distance from, the vibration source, the soilbag-based reinforcement had a lower peak acceleration and a higher attenuation rate than the geogrid-based reinforcement and the unreinforced subgrade. That is, the soilbag structure best resisted transmission vibrations. Researcher has suggested that the extension and contraction of the bag as well as the frictional motion of the soil particles inside it play a significant role in dissipating vibrational energy during cyclic loading and unloading (Matsuoka and Liu, 2006). The more effective vibration reduction brought about by using the soilbag-based reinforcement can also be attributed to gaps between soilbags where vibration waves could not be transmitted.

3.2 Influence of cyclic load frequency

To investigate the influence of the frequency of cyclic loads, plate load tests were performed on a model subgrade reinforced with two layers of soilbags under a loading amplitude of 500 kPa at frequencies of 0.5 Hz, 1 Hz, and 1.5 Hz, respectively. Figure 7 shows the evolution of the permanent and resilient deformations of the model subgrade during repeated loadings under different frequencies. It shows that for any given number of applications, a higher cyclic loading frequency produced a greater permanent deformation. On the contrary, the resilient deformation of the subgrade decreased with an increase in load frequency, meaning that the resilient modulus of the subgrade and, consequently, the capacity of resistance to settlement increased. This is because

the increase in the frequency of cyclic loading accelerated the dynamic impulse of the load on the subgrade. At higher frequencies, the particle rearrangement could not match the dynamic impulse, resulting in a lower resilient (recoverable) deformation and larger plastic (unrecoverable) deformation.

The influence of the frequency of cyclic load on the peak acceleration and the decrease in it with depth and horizontal distance from the source of vibration are shown in Figure 8. As expected, the increase in the frequency of load led to an increase in the peak acceleration of the subgrade, especially near the source of vibration (circular load plate). The ratio of attenuation generally increased with frequency.

3.3 Effect of cyclic load amplitude

The evolution of permanent (settlement) and resilient deformations of the two-layer soilbag-reinforced subgrade subjected to cyclic load at a frequency of 1 Hz, and amplitudes of 250 kPa, 500 kPa, and 750 kPa, are shown in Figure 9. Both the permanent deformation and the resilient deformation increased with amplitude. After 1,000 cycles, the measured permanent deformations of the model subgrade were 13.84 mm, 23.22 mm, and 30.51 mm at amplitudes of 250 kPa, 500 kPa, and 750 kPa, respectively. Correspondingly, the resilient deformations of the model subgrade were 0.58 mm, 0.95 mm, and 1.19 mm. Using this, the resilient modulus of the model subgrade after 1,000 cycles were back-calculated using Equation (1) to be 128, 155, and 182 MPa. This illustrates that the resilient modulus of the model subgrade improved, although the increase in the amplitude of load increased the settlement. Figure 9(b) also shows that the resilient deformation decreased with the number of loading cycles in each test, resulting in an increase in the resilient modulus. The increase in the resilient modulus with the both the amplitude of load and the number of loading cycles suggests that the soilbag-based reinforcement helped prevent the generation of cracks in the road pavement under heavy traffic loads.

Figure 10 shows the variation in the peak acceleration (PA) and rate of attenuation (AR) of the model subgrade with depth and horizontal distance at amplitudes of 250, 500, and 750 kPa. The peak acceleration increased with amplitude, especially near the vibration source (15 cm in depth and at a 25 cm horizontal surface distance). However, the influence of the amplitude of load on the attenuation rate was not prominent in the tests, except for the higher AR near the vibration source.

3.4 Effect of number of soilbag layers

Three tests were conducted on the model subgrade reinforced with one, two, and three layers of soilbags at an amplitude of 500 kPa and frequency of 1 Hz. Each model in each test was 750 mm high, and the first layer was placed 5 cm beneath the surface. The results are given in Figures 11 and 12. As shown in Figure 11, both the permanent and the resilient deformations of the model subgrade decreased with increase in the number of soilbag-reinforced layers. The reinforcement with one layer of soilbags yielded the most significant permanent deformation of 27.85 mm after 1,000 cycles, whereas the reinforcement with three layers of soilbags led to the lowest permanent deformation of 22.23 mm. However, the increment in the permanent deformation between the two- and three-layer reinforcements was not as significant as that between the one- and two-layer reinforcements. This can be interpreted as the effect of the interlayer insertion of soilbags, as illustrated in the inset of Figure 11(a). When the soilbags were arranged in a staggered manner, the flexible soilbag in the upper layer deformed to form gaps between soilbags in the lower layer, with embedded contacts when subjected to vertical load (Fan et al. 2020a, b). No interlayer insertion was observed in the one-layer reinforcement. In case of two- and three-layer reinforcements, the interlayer insertion increased interlayer frictional resistance and thus enhanced the integrity of the reinforced layers. Furthermore, Figure 11(b) shows the tendency of the decrease in resilient deformation (i.e. the increase in resilient modulus) during cyclic loading in the cases of two- and three-layer reinforcements compared with that of the one-layer reinforcement. With an increase in the number of soilbag layers, the peak acceleration of the model subgrade decreased both along the depth and the horizontal distance, as shown in Figure 12. Near the source of the vibration (a depth of 15 cm and horizontal surface distance of 25 cm), the three-layer reinforcement had the largest rate of attenuation. These test results suggest that more than two layers of soilbags are needed as reinforcement for the road subgrade.

3.5 Effect of buried depth of soilbag reinforcement

Research has shown that the embedded depth of geosynthetics reinforcements influences the bearing capacity as well as other properties of geosynthetic-reinforced subgrades (e.g. Pokharel et al. 2010). The effect of the buried depth of soilbag-based reinforcements has also been investigated through cyclic plate load tests on model subgrades reinforced with two layers of soilbags embedded at different depths (0 cm, 5 cm, 10 cm, and 15 cm). The amplitude and the frequency of load in the tests were 500 kPa and 1 Hz, respectively. The test results are given in Figures 13 and 14, where “u” denotes the buried depth of the first layer of soilbag-based reinforcement beneath the loading plate.

As is shown in Figure 13, the increase in the permanent and resilient deformations of the subgrade was small as the buried depth u increased from 0 cm to 5 cm, but the settlement was prominent as the buried depth u increased from 5 cm to 15 cm. The slight increase in the deformation of the subgrade at a buried depth of u = 5 cm can be attributed to the behaviour of the surface layer of soil between the load plate and the first layer of the soilbags. When the buried soilbag reinforcements were thin, the surface sand layer acted as a cushion to provided load spreading without significant lateral deformation. However, if the buried depth u became too large, particles within the surface layer of soil were displaced, causing larger permanent and resilient deformations. In road engineering, a thin surface soil cover is desirable for subgrade levelling. Figure 14 shows variations in the peak acceleration and attenuation rate of the model subgrade with depth and horizontal displacement, corresponding to different buried depths of the first layer of soilbags. Overall, the peak acceleration increased with the buried depth at the same location, although the change in the attenuation rate was not prominent for different buried depths. These results indicate that a shallow embedded depth provides effective settlement resistance and reduction in vibration.

4. CONCLUSIONS

In this study, the use of soilbags as reinforcement in road subgrades under traffic loads was investigated through cyclic plate load tests on a model subgrade. The tests compared the model subgrade reinforced with geogrids with that without a reinforcement. The influence of the frequency and amplitude of cyclic loading, the number of layers of soilbags, and the embedded depths was examined on the performance of the model subgrade. The main results can be summarized as follows:

(1) The reinforcement with soilbags significantly reduced the permanent deformation (settlement) and resilient deformation of the road subgrade as well as vibrations under repeated loading. Owing to the three-dimensional confinement of the soilbags, the reinforcement based on them was more effective than the geogrid-based reinforcement when the same number of reinforcement layers were used.

(2) The performance of the soilbag-based reinforcement was affected by cyclic frequency and load amplitude. The settlement and peak acceleration of the subgrade increased with the cyclic frequency and amplitude of load during repeated loading. However, the resilient modulus of the subgrade increased with both the amplitude of load and the number of loading cycles at the same cyclic frequency, suggesting that the soilbag-based reinforcement can protect against cracks in road pavements subjected to heavy traffic loads.

(3) The performance of the soilbag-based reinforcement improved when the number of soilbag-reinforced layers increased. To make use of the effect of interlayer insertion among soilbags, more than two layers of them are needed to reinforce road subgrades.

(4) The relatively shallow embedded depth of the soilbag-based reinforcement provided effective settlement resistance and a reduction in vibration. However, the thin surface soil cover was desirable for spreading the applied pressure to a greater extent over the soilbag-based reinforcement, and to level the subgrade.

ACKNOWLEDGEMENTS

This study was supported by the National Key R&D Program of China (Grant No. 2017YFE0128900), and the National Natural Science Foundation of China (Grant No. 51379066).

LIST OF NOTATION

Basic SI units are given in parentheses.

E resilient modulus (Pa)

B diameter of the loading plate (m)

I influence factor of the load plate (dimensionless)

q pressure applied on surface of the subgrade (Pa)

ν Poisson's ratio (dimensionless)

δ resilient deformation (m)

AR attenuation rate of subgrade (dimensionless)

a_{max}^{i} peak acceleration at the measuring point i (m/s^2)

a_{max}^{i-1} peak acceleration at the measuring point i-1(m/s^2)

REFERENCES

Cheng, H.Y., Yamamoto, H. & Thoeni, K. (2016). Numerical study on stress states and fabric anisotropies in soilbags using the DEM. *Computers and Geotechnics*, **76**: 170-183.

Ding, G.Y., Wu, J.L., Wang, J. & Hu, X.Q. (2017). Effect of sand bags on vibration reduction in road subgrade. *Soil Dynamics and Earthquake Engineering*, **100**: 529–537.

Ding, G.Y., Wu, J.L., Wang, J., Fu, H.T. & Liu, F.Y. (2018). Experimental study on vibration reduction by using soilbag cushions under traffic loads. *Geosynthetics International*, **25**: 322–333.

Ding, G.Y., Guan, C.D. & Wang. J. (2018). Vibration reduction using wave barrier: model test and theoretical analysis. *Geotechnical and Geological Engineering*, **37(3)**: 2065-2080.

Fan, K., Liu, S. H., Cheng, Y. P., & Wang, Y. (2019). Sliding stability analysis of a retaining wall constructed by soilbags. *Géotechnique Letters*, **9(3)**, 211-217.

Fan, K.W., Liu, S.H., Liao, J., Fang, B.X. & Wang, L. J. (2020). Experimental studies on shearing characteristics of the pebbles-filled soilbags. *Chinese Journal of Rock Soil Mechanics*. **41**: 1–8 (in Chinese).

Fan, K., Liu, S., Cheng, Y. P., & Liao, J. (2020). Effect of infilled materials and arrangements on shear characteristics of stacked soilbags. *Geosynthetics International*, 1-30 (online).

Hanazato, T., Ugai, K., Mori, M. & Sakaguchi, R. (1991). Three-dimensional analysis of traffic-induced ground vibrations. *Journal of Geotechnical Engineering*, **117**: 1133–1151.

Hornsey, W.P., Carley, J.T., Coghlan, I.R. & Cox, R.J., 2011. Geotextile sand container shoreline protection systems: design and application. *Geotextiles and Geomembranes*, **29**: 425-439.

Indraratna, B., Biabani, M.M. & Nimbalkar, S. (2014). Behavior of geocell-reinforced subballast subjected to cyclic loading in plane-strain condition. *Journal of Geotechnical and Geoenvironmental Engineering*, **141**: 04014081.

JTG D50–2017. *Specifications for Design of Highway Asphalt Pavement*. China Communications Press, Beijing (in Chinese).

Kim, H.J., Won, M.S., Lee, K.H. & Jamin, J.C. (2015). Model tests on dredged soil-filled geocontainers used as containment dikes for the Saemangeum reclamation project in South Korea. *International Journal of Geomechanics*, **16(2)**: 04015055.

Lee, S.M., Choi, C. & Shin, E.C. (2013). A study of connection stability for reinforced retaining wall constructed with soilbag with varying connection strength. *Journal of the Korean Geosynthetics Society*, **12(1)**: 101–107.

Ling, J., Wei, W. & Hongbo, W. (2002). On residual deformation of saturated clay subgrade under vehicle load. Journal-Tongji University, **30**: 1315–1320(in Chinese).

Li, Z., Liu, S.H., Wang, L.J. & Zhang, C.C. (2013). Experimental study on the effect of frost heave prevention using soilbags. *Cold Regions Science and Technology*, **85**: 109-116.

Liu, S.H., Bai, F.Q., Wang, Y.S., Wang, S. & Li, Z. (2013). Treatment for expansive soil channel slope with soilbags. *Journal of Aerospace Engineering*, **26**: 657–666.

Liu, S.H. (2017). *Principle and application of soilbags. Science Press*, Beijing (in Chinese).

Liu, S.H., Gao, J.J., Wang, Y.Q. & Weng, L.P. (2014). Experimental study on vibration reduction by using soilbags. *Geotextiles and Geomembranes*, **42**: 52–62.

Liu, S.H., Lu, Y., Weng, L.P. & Bai, F.Q. (2015). Field study of treatment for expansive soil/rock channel slope with soilbags. *Geotextiles and Geomembranes*, **43**: 283–292.

Liu, S.H. & Matsuoka, H. (2007). A new earth reinforcement method by soilbags. *Chinese Journal of Rock Soil Mechanics*, **28**: 1665-1670 (in Chinese).

Liu S.H., Fan K.W. & Xu S.Y. (2019). Field study of a retaining wall constructed with clay-filled soilbags. *Geotextiles and Geomembranes*, **47**: 87–94.

Matsuoka, H. & Ando, T. (2006). Reduction of road traffic-induced vibration by layered soilbags (Donow). *Doboku Gakkai Ronbunshu*. **62(2)**: 379–89 (in Japanese).

Matsuoka, H. & Liu, S. H. (1999). Bearing capacity improvement by wrapping a part of foundation. *Doboku Gakkai Ronbunshu*, **617**: 235-249 (in Japanese).

Matsuoka, H. & Liu, S. H. (2003). New earth reinforcement method by soilbags (Donow). *Soils and Foundations*. **43(6)**: 173–188.

Matsuoka, H. & Liu, S.H. (2006). *A New Earth Reinforcement Method Using Soilbags*.Taylor & Francis/Balkema, The Netherlands.

Matsuoka, H., Liu, S.H., Kodama, H. & Kachi,T. (2000). Reduction of settlement for ballast foundation under railway sleepers by soilbags. *Proceedings of the 35th Japan National Conf. on Geotechnical Engineering*, **547**, pp. 1081-1082 (in Japanese).

Matsuoka, H., Liu, S.H., Muramatu, D., Inoue, T., Andou, H., Asano, K. & Taniguchi, N. (2003). Reduction of traffic-induced vibration by soilbags. *Proceedings of the 38th Japan National Conf. on Geotechnical Engineering*, **658**, pp. 1098-1100 (in Japanese).

Matsuoka, H., Liu, S.H., Yamamoto, H., Satoh, M., Tatsui, T. & Matsumoto, T. (2002). Vibration reduction tests at a construction road in G-city. *Proceedings of the 37th Japan National Conf. on Geotechnical Engineering*. **458**, pp. 981-982 (in Japanese).

Matsuoka, H. & Nomoto, F. (2008). Local consolidation and reinforcement method for ultra-weak foundation with soilbags. *Proceedings of the 43th Japan National Conf. on Geotechnical Engineering*. **301**, pp. 601-602 (in Japanese).

Mehrjardi, G. T., Ghanbari, A., & Mehdizadeh, H. (2016). Experimental study on the behaviour of geogrid-reinforced slopes with respect to aggregate size. *Geotextiles and Geomembranes*, **44(6)**, 862-871.

Martinelli, L., Zanuttigh, B., De Nigris, N. & Preti, M. (2011). Sand bag barriers for coastal protection along the Emilia Romagna littoral, Northern Adriatic Sea, Italy. *Geotextiles and Geomembranes*, **29 (4)**: 370-380.

Moreira, A., Vieira, C.S., das Neves, L. & Lopes, M.L. (2016). Assessment of friction properties at geotextile encapsulated-sand systems' interfaces used for coastal protection. *Geotextiles and Geomembranes*, **44**: 278-286.

Monismith, C.L., Ogawa, N. & Freeme, C.R. (1975). Permanent deformation characteristics of subgrade soils due to repeated loading. *Transportation Research Record*, 537.

Nakagawa, Y., Chen, G. L., Tatsui, T. & Chida, S. (2009). Verification of vibration reduction characteristics with soilbag structure. *Proceedings of the 4th Asian Regional Conference on Geosynthetics*, Shanghai, China, Springer-Verlag, Berlin, Heidelberg, Germany, pp. 603–608.

Pokharel, S.K., Han, J., Leshchinsky, D., Parsons, R.L. & Halahmi, I. (2010). Investigation of factors influencing behavior of single geocell-reinforced bases under static loading. *Geotextiles and Geomembranes*, **28**: 570–578.

Qian, Y., Han, J., Pokharel, S.K. & Parsons, R.L. (2011). Stress analysis on triangular-aperture geogrid-reinforced bases over weak subgrade under cyclic loading: An experimental study. *Transportation Research Record*, **2204**: 83–91.

Shao, J.X., Huang, J. & Zhou, B.M. (2005). Application of soilbags in subgrade engineering. *Highway* **7**, 82–86 (in Chinese).

Saad, B., Mitri, H. & Poorooshasb, H. (2005). Three-dimensional dynamic analysis of flexible conventional pavement foundation. *Journal of* Transportation Engineering, **131**: 460–469

Suku, L., Prabhu, S.S., Ramesh, P. & Babu, G.L.S. (2016). Behavior of geocell-reinforced granular base under repeated loading. *Transportation Geotechnics*, **9**: 17–30

Suku, L., Prabhu, S.S. & Sivakumar Babu, G.L. (2017). Effect of geogrid-reinforcement in granular bases under repeated loading. *Geotextiles and Geomembranes*, **45**: 377–389.

Tafreshi, S.N.M. & Dawson, A.R. (2010). Behaviour of footings on reinforced sand subjected to repeated loading - Comparing use of 3D and planar geotextile. *Geotextiles and Geomembranes*, **28**: 434–447.

Tafreshi, S.N.M., Khalaj, O. & Dawson, A.R. (2014). Repeated loading of soil containing granulated rubber and multiple geocell layers. *Geotextiles and Geomembranes*, **42**: 25–38.

Tantono, S.F. & Bauer, E. (2008). Numerical simulation of a soilbag under vertical compression. *In Proceeding of the 12th International Conference of International Association for Computer Methods and Advances in Geomechanics*, Goa, India, pp. 433–439.

Thakur, J.K., Han, J., Pokharel, S.K. & Parsons, R.L. (2012). Performance of geocell-reinforced recycled asphalt pavement (RAP) bases over weak subgrade under cyclic plate loading. *Geotextiles and Geomembranes*, **35**: 14–24.

Wang, J. Q., Zhang, L.L., Xue, J.F. & Tang, Y. (2018). Load-settlement response of shallow square footings on geogrid-reinforced sand under cyclic loading. *Geotextiles and Geomembranes*, **46**: 586–596.

Wang, L.J., Liu, S.H., Liao, J. & Fan, K.W. (2019). Field load tests and modelling of soft foundation reinforced by soilbags. *Geosynthetics International*, **24(6)**, 580-591.

Wang, L.J., Liu, S.H. & Zhou, B. (2015). Experimental study on the inclusion of soilbags in retaining walls constructed in expansive soils. *Geotextiles and Geomembranes*, **43(1)**: 89-96

Wang, Y.Q. & Wang, L.J. (2014). Numerical simulation of vibration reduction and energy dissipation of soilbags. *Chinese Journal of Rock Soil Mechanics*, **35(2)**: 601–606 (in Chinese).

Wang, Y. Q., Liu, K., Li, X., Ren, Q. B., Li, L. L., Zhang, Z. H., & Li, M. C. (2019). Experimental and upper-bound study of the influence of soilbag tail length on the reinforcement effect in soil slopes. Geotextiles and Geomembranes, **47(5)**, 610-617.

Wang, Y. Q., Li, X., Liu, K., & Liu, G. (2019). Experiments and DEM analysis on vibration reduction of soilbags. Geosynthetics International, **26(5)**, 551-562.

Wen, H., Wu, J., Zou, J., Luo, X., Zhang, M. & Gu, C. (2016). Model tests on the retaining walls constructed from geobags filled with construction waste. *Advances in Materials Science and Engineering*, 2016.

Xu, Y.F., Huang, J., Du, Y.J. & Sun, D.A. (2008). Earth reinforcement using soilbags. *Geotextiles and Geomembranes*, **26**: 279-289.

Yamamoto, H., Matsuoka, H., Simao, R., Hasebe, T. & Hattori, M. (2003). Cyclic shear property and damping ratio of soilbag assembly. *In Proceedings of the 38th Japan National Conference on Geotechnical Engineering*, Japan, pp. 757-758.

Ye, B., Muramatsu, D., Ye, G.L. & Zhang, F. (2011). Numerical assessment of vibration damping effect of soilbags. *Geosynthetics International*, **18**: 159-168.

Table Captions

Table 1. Properties of the subgrade and the filling material.

Table 2. Testing arrangement.

Table 1. Properties of the subgrade and the filling material.

Medium grain diameter, D_{50} (mm)	0.36
Coefficient of uniformity, C_u	1.98
Coefficient of curvature, C_c	1.02
Minimum dry density, ρ (g/cm^3)	1.45
Maximum dry density, ρ (g/cm^3)	1.72
Water content, w (%)	5.0
Cohesion, c (kPa)	3.25
Internal friction angle, φ (°)	35.4

Table 2 Testing arrangement

Test series	Reinforcement	Layers	Buried depth (cm)	Amplitude of repeated load (kPa)	Load frequency (Hz)	Purpose of the tests
A	Unreinforced	/	/	500	1.0	To quantify the effectiveness of soilbags
	Soilbags	3	5	500	1.0	
	Geogrids	3	5	500	1.0	
B	Soilbags	2	5	500	0.5, 1.0, 1.5	To study the effect of dynamic load frequency
C	Soilbags	2	5	250, 500, 750	1.0	To study the effect of dynamic load amplitude
D	Soilbags	3, 2, 1	5	500	1.0	To study the effect of the number of soilbag layers
E	Soilbags	2	0, 5, 10, 15	500	1.0	To study the effect of the buried depth of soilbags

Accepted manuscript doi:
10.1680/jgein.20.00030

Figure Captions

Figure 1. Setup of soilbag-reinforced subgrade under cyclic load tests.

Figure 2. Geometry of the tested road subgrade model: (a) reinforced with soilbags; (b) reinforced with geogrids.

Figure 3. Components of repeated loading and deformation.

Figure 4. Vertical displacement of the loading plate vs. number of cycles for different types of reinforcements under a loading amplitude of 500 kPa and frequency of 1 Hz: (a) permanent deformation; (b) plastic deformation; (c) resilient deformation.

Figure 5. Acceleration response of the soilbag-reinforced model subgrade measured at different depths under repeated loading: (a) 5 cm depth; (b) 15 cm depth; (c) 25 cm depth; (d) 35 cm depth.

Figure 6. Variation in peak acceleration and ratio of attenuation in acceleration: (a) varying with depth; (b) varying with horizontal distance.

Figure 7. Deformation response of model subgrade under different frequencies of cyclic load: (a) permanent deformation; (b) resilient deformation.

Figure 8. Peak acceleration (PA) and attenuation ratio (AR) under different frequencies of cyclic load: (a) varying with depth; (b) varying with horizontal distance.

Figure 9. Deformation response of model subgrade under different amplitudes of cyclic load: (a) permanent deformation; (b) resilient deformation.

Figure 10. Peak acceleration (PA) and attenuation ratio (AR) under different amplitudes of cyclic load: (a) varying with depth; (b) varying with horizontal distance.

Figure 11. Deformation response of model subgrade reinforced with different layers of soilbags: (a) permanent deformation; (b) resilient deformation.

Figure 12. Peak acceleration (PA) and attenuation ratio (AR) of model subgrade reinforced with different layers of soilbags: (a) varying with depth; (b) varying with horizontal distance.

Figure 13. Deformation response of model subgrade reinforced with two layers of soilbags at different buried depths: (a) permanent deformation; (b) resilient deformation.

Figure 14. Peak acceleration (PA) and attenuation ratio (AR) of model subgrade reinforced with two layers of soilbags at different buried depths: (a) varying with depth; (b) varying with horizontal distance.

Accepted manuscript doi:
10.1680/jgein.20.00030

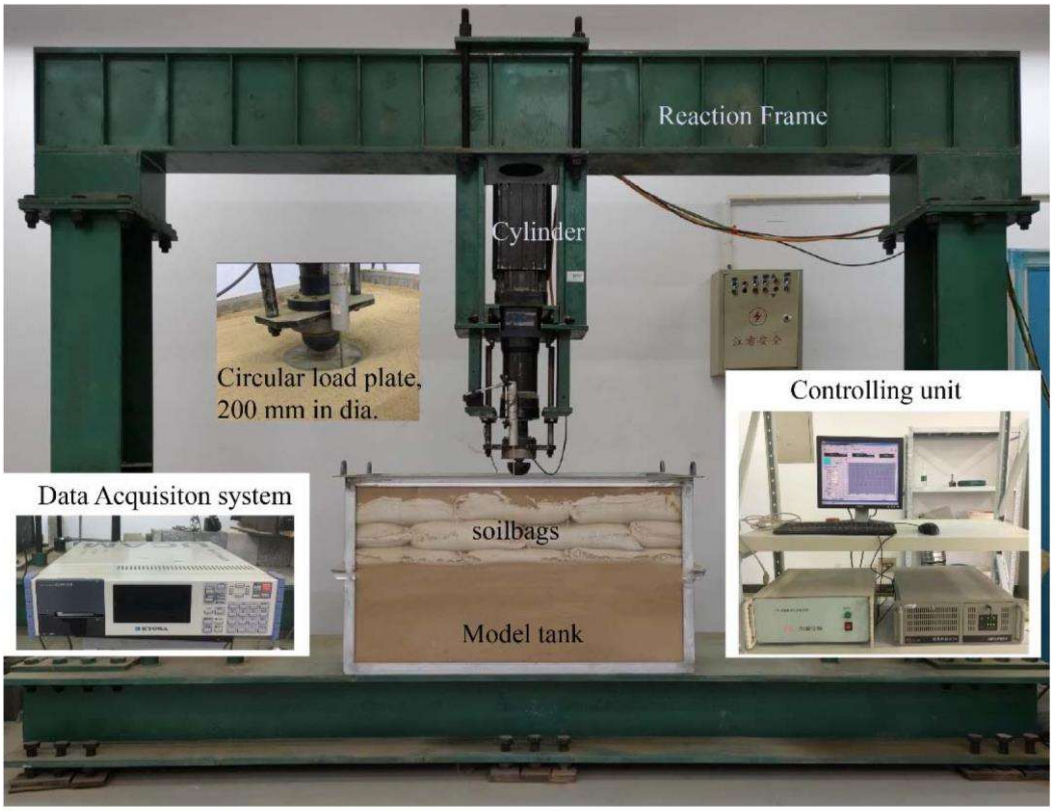

Figure 1

Accepted manuscript doi:
10.1680/jgein.20.00030

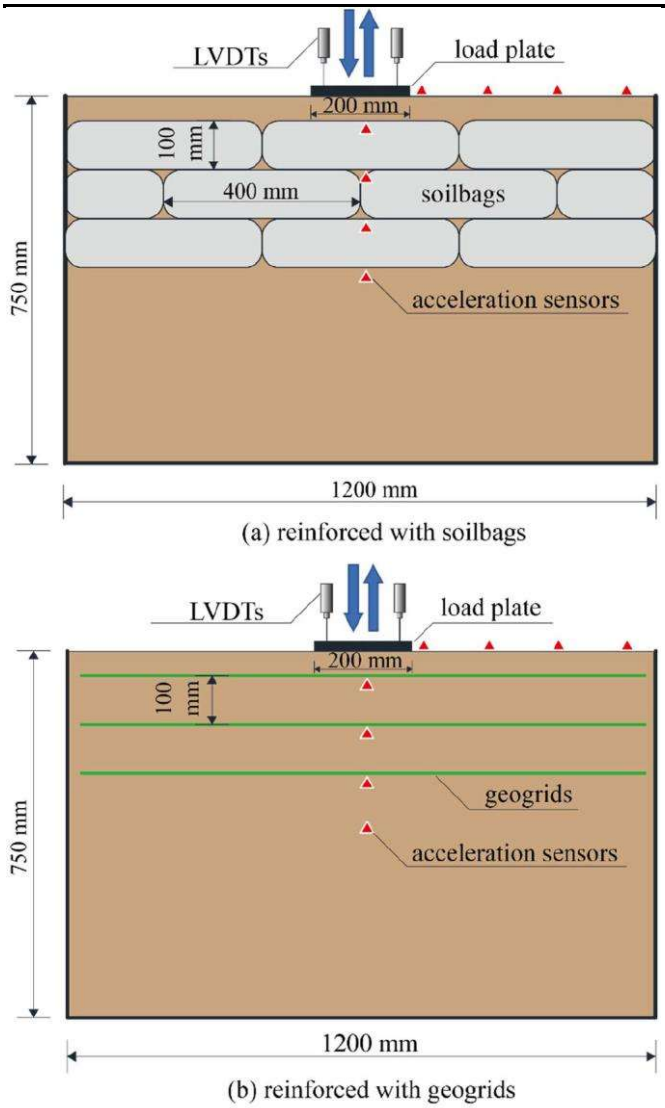

Figure 2

Accepted manuscript doi:
10.1680/jgein.20.00030

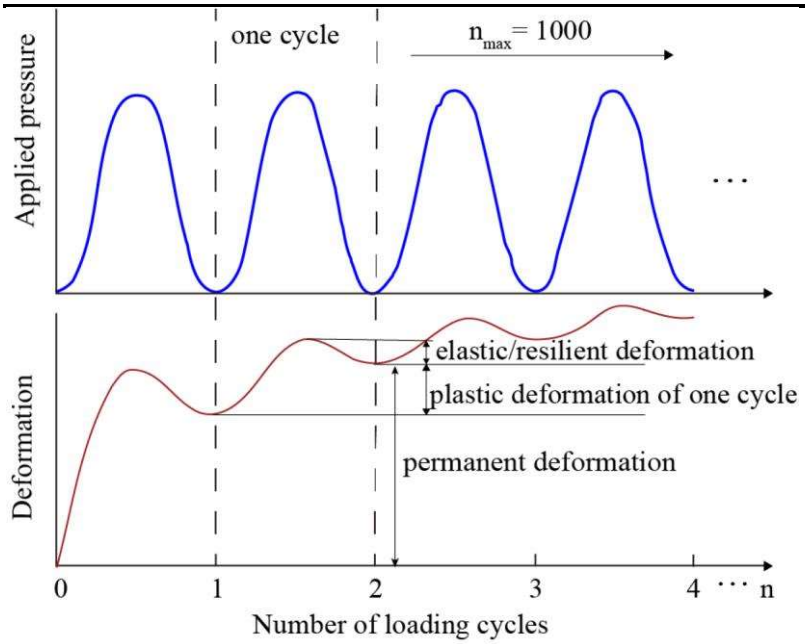

Figure 3

Accepted manuscript doi:
10.1680/jgein.20.00030

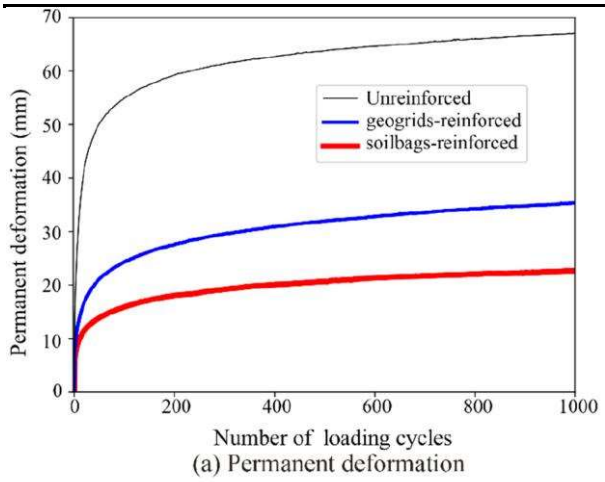

(a) Permanent deformation

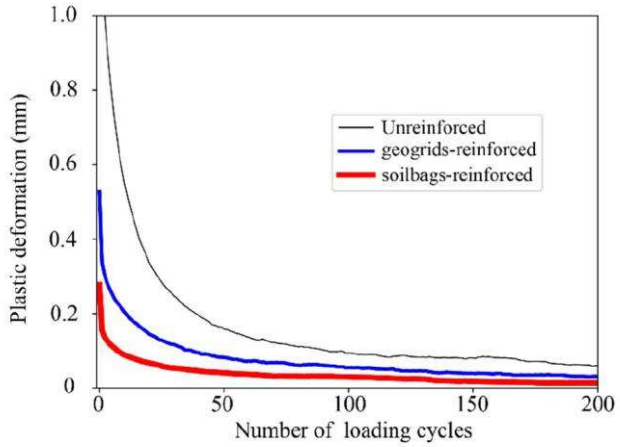

(b) Plastic deformation

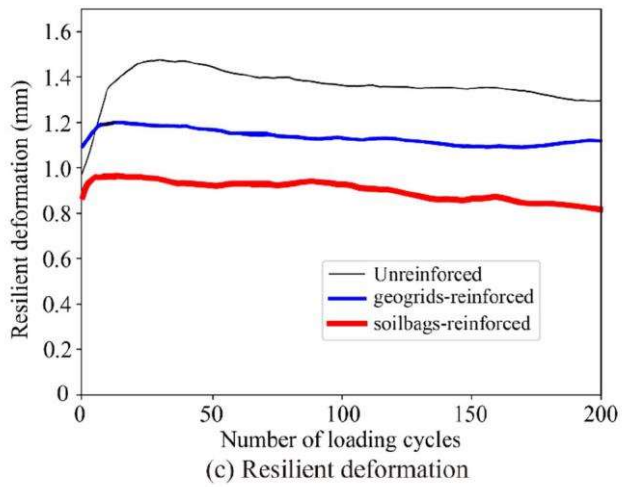

(c) Resilient deformation

Figure 4

Accepted manuscript doi:
10.1680/jgein.20.00030

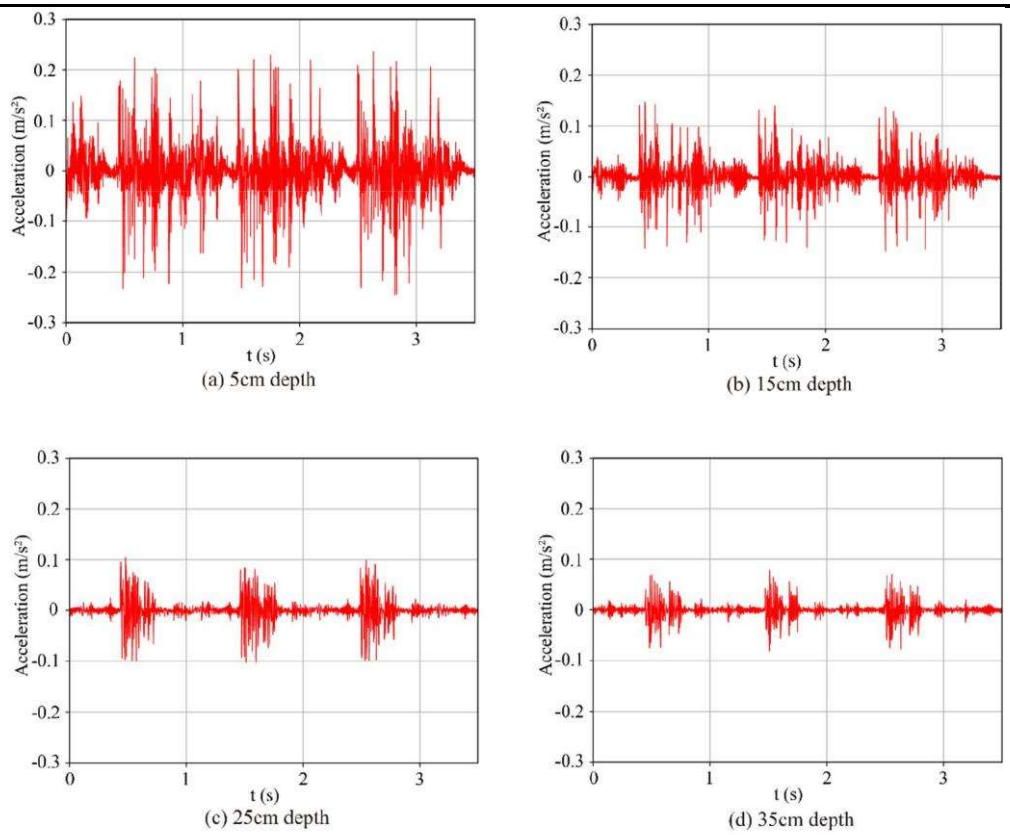

Figure 5

Accepted manuscript doi:
10.1680/jgein.20.00030

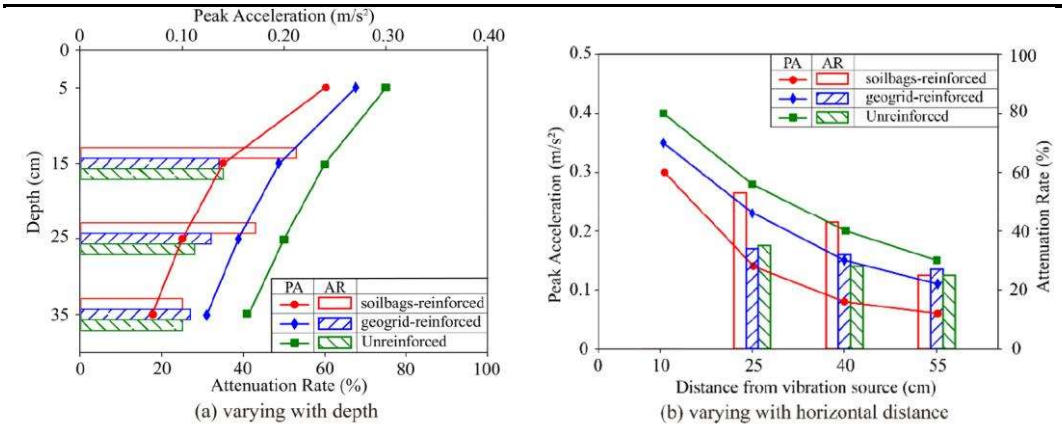

Figure 6

Accepted manuscript doi:
10.1680/jgein.20.00030

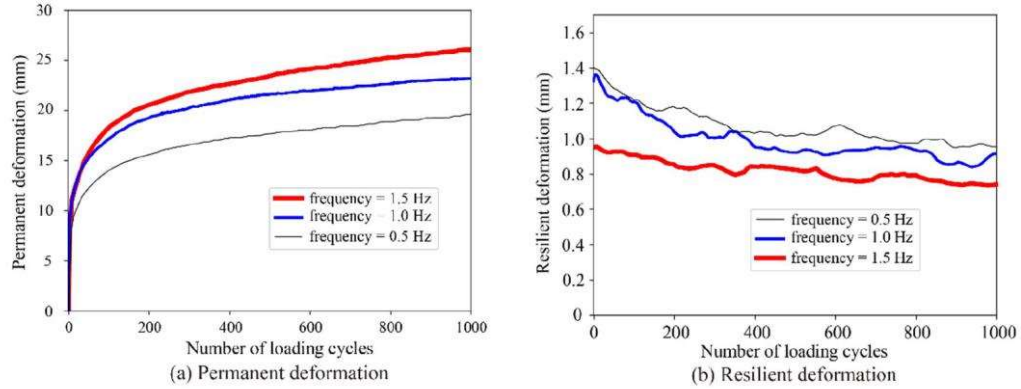

Figure 7

Accepted manuscript doi:
10.1680/jgein.20.00030

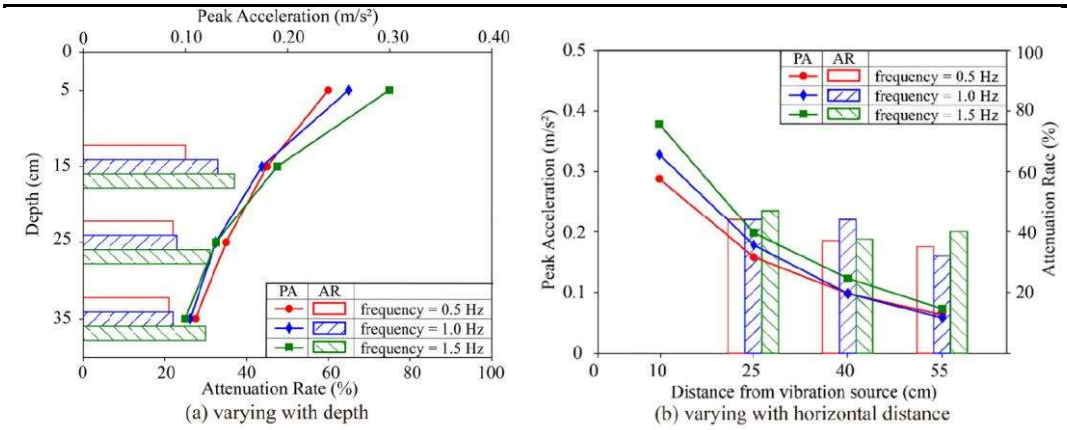

Figure 8

Accepted manuscript doi:
10.1680/jgein.20.00030

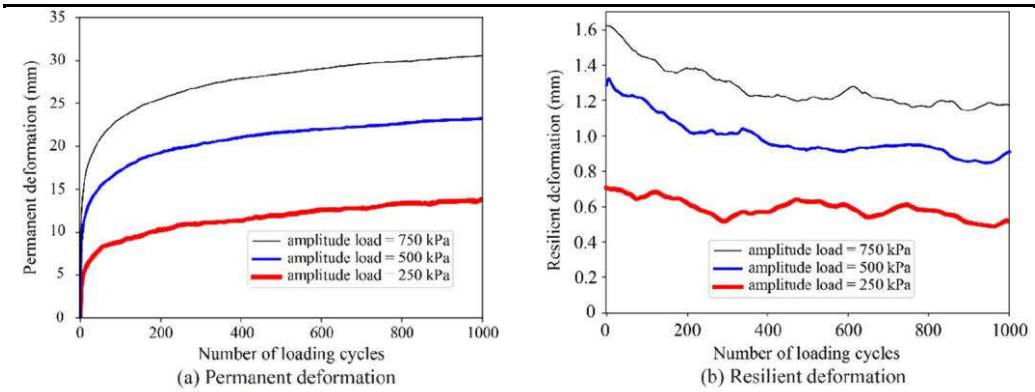

(a) Permanent deformation

(b) Resilient deformation

Figure 9

Accepted manuscript doi:
10.1680/jgein.20.00030

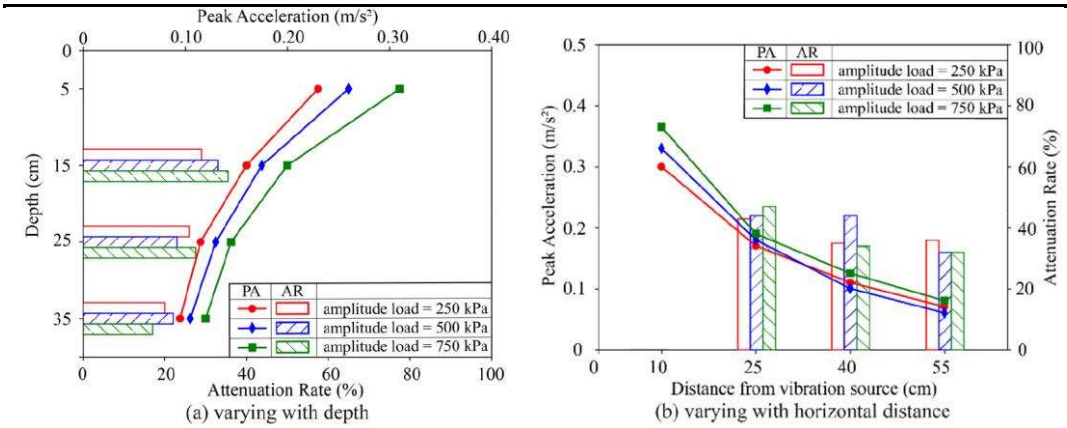

Figure 10

Accepted manuscript doi:
10.1680/jgein.20.00030

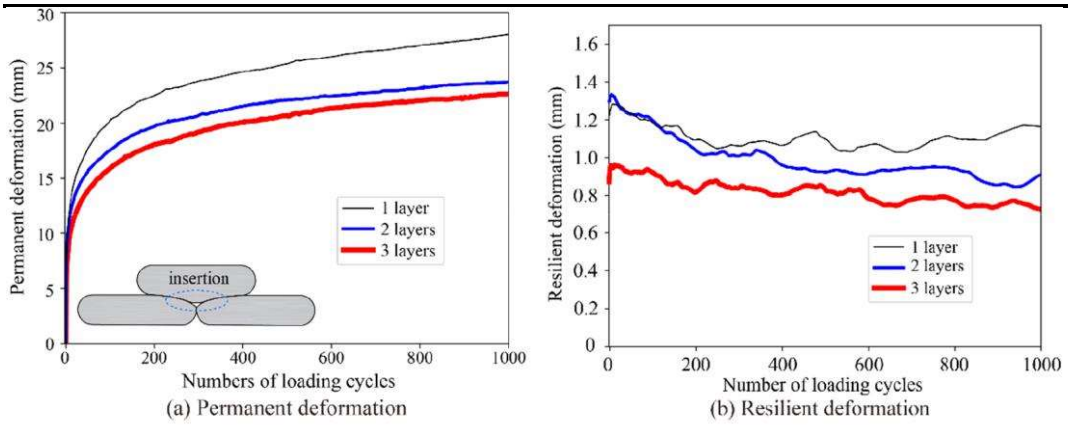

Figure 11

Accepted manuscript doi:
10.1680/jgein.20.00030

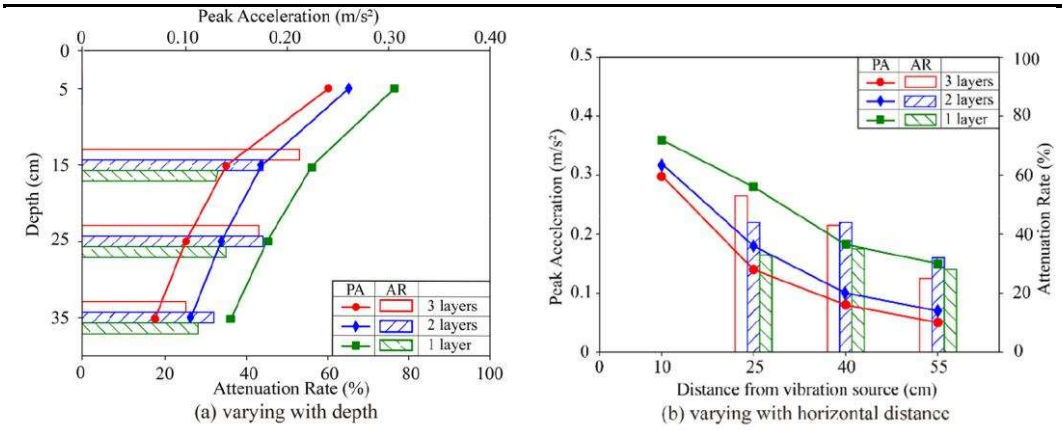

Figure 12

Accepted manuscript doi:
10.1680/jgein.20.00030

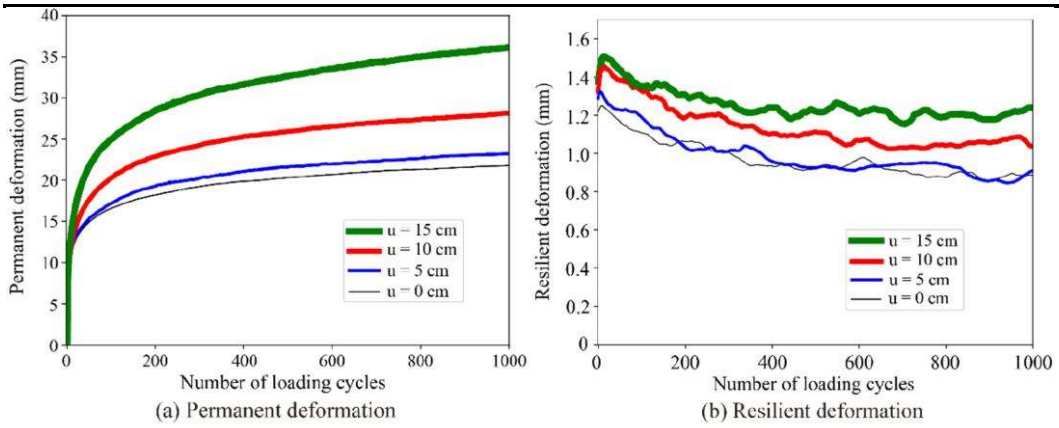

Figure 13

Accepted manuscript doi:
10.1680/jgein.20.00030

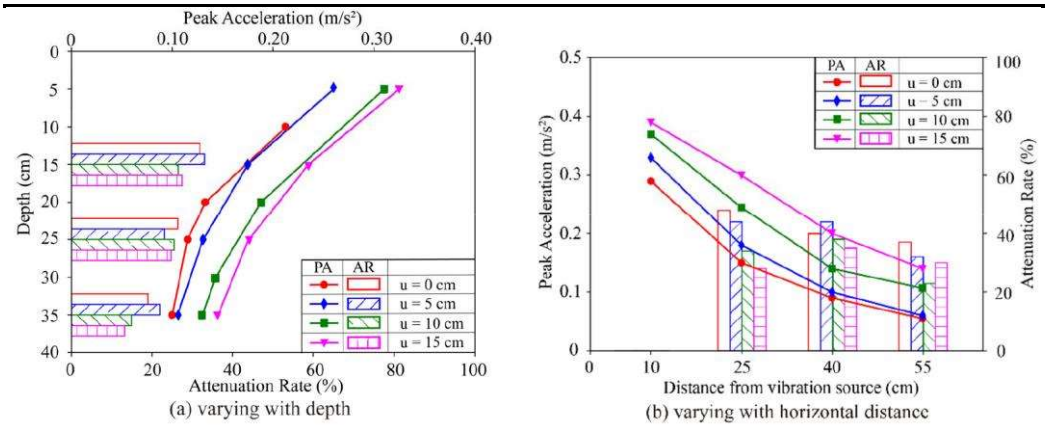

Figure 14